Macroscopic probabilistic cracking approach for the numerical modelling of fluid leakage in concrete

Giuseppe Rastiello, Jean-Louis Tailhan, Pierre Rossi, Stefano Dal Pont

Ann. Solid Struct. Mech. manuscript No.
(will be inserted by the editor)

Macroscopic probabilistic cracking approach for the numerical modelling of fluid leakage in concrete

Giuseppe Rastiello · Jean-Louis Tailhan · Pierre Rossi · Stefano Dal Pont

Received: date / Accepted: date

The final publication is available at http://link.springer.com/article/10.1007/s12356-015-0038-6

Abstract The article presents a numerical finite element study of fluid leakage in concrete. Concrete cracking is numerically modelled in the framework of a macroscopic probabilistic approach. Material heterogeneity and the related mechanical effects are taken into account by defining the elementary mechanical properties according to spatially uncorrelated random fields. Each finite element is considered as representative of a volume of heterogeneous material, whose mechanical behaviour depends on its own volume. The parameters of the statistical distributions defining the elementary mechanical properties thus vary over the computational mesh element-by-element. A weak hydro-mechanical coupling assumption is introduced to represent the influence of cracking on the variation of transfer properties: it is assumed that the mechanical cracking of a finite element induces a loss of isotropy of its own permeability tensor. At the elementary level, an experimentally enhanced parallel plates model is used to relate the local crack permeability to the elementary crack aperture. A Monte Carlo-like approach allows to statistically validate the numerical method. The self-consistency of the proposed modelling strategy is finally explored through the numerical simulation of the hydro-mechanical splitting test, recently proposed by Authors to evaluate the real-time evolution of the transfer properties of a concrete sample under loading.

Keywords concrete cracking · concrete heterogeneity · probabilistic model · weak hydro-mechanical coupling · modified cubic law · splitting test

G. Rastiello · J.-L. Tailhan · P. Rossi · S. Dal Pont
Université Paris-Est, IFSTTAR, 14-20 Boulevard Newton, Cité Descartes, Champs-sur-Marne, F-77447 Marne la Vallée Cedex 2, France
Present address: G. Rastiello, LMT (ENS Cachan / CNRS / Université Paris Saclay), 61 Avenue du Président Wilson, 94235 Cachan, France, E-mail: g.rastiello@gmail.com, rastiello@lmt.ens-cachan.fr
S. Dal Pont, CNRS / UJF / INPG, Laboratoire 3SR, BP53, Domaine Universitaire, 38041 Grenoble, France

1 Introduction

Fluids (gas, water, aggressive agents, ...) may penetrate through concrete due to its porous structure and to micro/macro cracks. Strictly related to the concrete heterogeneous nature, their presence is inevitable even in the presence of small loading levels or at early-age (Ulm and Coussy 1998; Sellier et al 2010; Briffaut et al 2011). This aspect is of crucial importance, because cracks represent preferential flow paths for the transport of fluid species, and strongly contributes to the deterioration of structural durability (Montemor et al 2003; Andrade and Gonzalez 2004; Millard and L'Hostis 2012) and safety (Granger et al 2001; Simon et al 2007; Dal Pont et al 2007).

Many numerical models aiming to model strain localisation and cracking in porous solids (e.g. concrete) have been proposed in the literature. Mainly developed in the framework of the Finite Element Method (FEM), from a conceptual point of view these formulations can be classified in relation to their modelling scale. In multiscale models (Segura and Carol 2004; Barani et al 2011; Carrier and Granet 2011; Secchi and Schrefler 2012; Larsson and Larsson 2000; Callari and Armero 2002; Réthoré et al 2007; Jourdain et al 2014), transport processes in porous material, the localised flow through

the discontinuity and their mutual exchanges are explicitly modelled. In macroscopic formulations (Bary 1996; Gawin et al 1999; Picandet 2001; Gawin et al 2002; Dal Pont et al 2005; Pijaudier-Cabot et al 2009) these phenomena are treated as a whole in the framework of the Theory of Porous Media (Lewis and Schrefler 1987; Coussy 2004). Each cracked volume element is then represented through an equivalent porous medium, with effective hydro-mechanical (HM) properties (i.e. Biot's coefficients, permeabilities, diffusivities, etc.) depending on the local mechanical fields (i.e. stress, strain, damage, crack opening, etc.).

Although multi-scale approaches allow for a more physical description of transport process in cracked domains (Bodin et al 2003), in particular when dealing with localised cracking, macroscopic formulations have been often preferred for engineering oriented applications. This is due to different reasons, and among others: they generally require lower computational ressources, their numerical implementation is quite simple, well established and validated thermodynamic frameworks are available, different physics can be coupled into a unified formulation in a natural way.

Whatever the finalities of the coupled modelling (e.g. prediction of fluid leakage through fluid containment structures, durability analysis of concrete structures) the model capabilities in predicting concrete cracking represent a key aspect.

Among the different mechanical models available in the literature, probabilistic formulations have proven to deal to a proper description of concrete. In these formulations, concrete heterogeneity and the related scale effects are taken into account by defining the material properties through random fields (Rossi and Wu 1992; Colliat et al 2007; Su et al 2010; Ibrahimbegovic et al 2011; Meftah et al 2012; Syroka-Korol et al 2013).

In particular, if the equivalence between a FE and a volume of heterogeneous material is postulated Rossi and Wu (1992), the use of spatially uncorrelated random fields allows for a relevant modelling of scale effects and cracking. Based on this original idea different numerical formulations have been developed in recent years (Rossi et al 1996; Tailhan et al 2010, 2012, 2013).

Drawing from these theoretical and numerical frameworks, a three-dimensional (3D) macroscopic modelling approach of fluid transfers in cracking concrete and concrete structures is presented in the paper.

The article is structured in three parts as follows:

1. a probabilistic mechanical model, developed in the FEM context, is first presented. In the present formulation, it is assumed that the cracking process (i.e. the creation and propagation of a crack within the element itself) induces some local energy dissipation. This dissipative process is mathematically represented through a probabilistic isotropic damage model. According to the aforementioned modelling assumption, material properties (strength and fracture energy) are defined element-by-element according to spatially uncorrelated random fields. Their statistical parameters are defined for each element depending on its own elementary volume according to experimentally validated laws;
2. the second part of the paper presents the coupled HM cracking-transfer modelling procedure. In this simplified formulation, the sole considered source of HM coupling is the influence of elementary cracking on the local variation of the transfer properties of the cracked volume. At the FE scale, this leads to consider that the localised flow through the crack induces a loss of isotropy in the elementary permeability tensor. The "apparent" elementary permeability is then computed through the experimentally adapted parallel plates model (Zimmerman and Bodvarsson 1996; Rastiello et al 2014);
3. in the final part of the article the self-consistency of the proposed approach is explored. For this purpose, the experimental HM test proposed by Rastiello et al (2014) to monitor the real-time evolution of the water permeability of a concrete sample under Brazilian loading is numerically modelled. Purely mechanical experimental results are used as reference data to calibrate the mechanical model parameters first. Then the HM response of cylindrical sample under mechanical and hydraulic loading is simulated.

2 Probabilistic cracking model

2.1 Problem setting

A macroscopic formulation for modelling pure tension (mode I) concrete cracking is presented. The probabilistic aspects of the model are based on the following fundamental modelling and physical assumptions (Rossi et al 1994; Tailhan et al 2010):

1. each FE is assumed to be representative of a volume of heterogeneous material, whose degree of heterogeneity ξ_e is defined as the ratio of its volume V_e to the volume of the coarsest aggregate V_g:

$$\xi_e = \frac{V_e}{V_g}\,; \tag{1}$$

2. the physical mechanisms controlling the cracking process are independent on the scale of modelling. Consequently, it is assumed that it is possible to define macroscopic quantities regardless of the size of

the FE, whether a Representative Elementary Volume (REV) or not;
3. the mechanical behaviour of each FE depends on its own volume and is prone to random variations. This aspect is represented by considering the elementary mechanical properties as randomly distributed over the computational mesh according to spatially uncorrelated random fields. Their statistical parameters thus vary element-by-element depending on the local heterogeneity ratio ξ_e;
4. crack propagation is not explicitly addressed, at least in the sense of the Fracture Mechanics. A propagation criterion is not introduced, but cracking is modelled element-by-element. The occurrence of a macro-crack (i.e. strain localisation) then results from the coalescence of some randomly created elementary cracks. In other words, at a macroscopic level, the progressive cracking of consecutive FEs is considered as representative of a macro-crack propagation.

According to these aspects, the presented approach is denoted in the following as "semi-explicit" instead of macroscopic. This term is here used to specify that, a discrete vision of cracking is preserved (the material's properties are discretely distributed in the mesh, the crack is treated element-by-element) but elementary cracking is taken into account through its local energetic effect.

2.2 Model formulation

Standard FEM procedures are used to solve quasi-static equilibrium equations. At the FE scale, the energetic effect associated to the elementary cracking process is represented through a simple isotropic damage law with a single scalar parameter (Lemaitre and Chaboche 1994). A probabilistic energetic regularisation is also retained.

Without going into details of numerical implementation of the model, its main features can be summarised as follows:

1. a bilinear stress-strain $(\boldsymbol{\sigma}, \boldsymbol{\varepsilon})$ relationship is used to represent elementary cracking (Fig. 1). The elementary dissipative process (i.e. crack propagation inside the FE itself) starts when the major principal stress $\sigma_{\max}^{prin}$ at a given Gauss point equals the material tensile strength f_t. Dissipation is then driven by the positive part, denoted by $\langle \bullet \rangle^+$, of the projection of $\boldsymbol{\varepsilon}$ along the direction $\mathbf{n}_\sigma$ of the major principal stress: $\tilde{\varepsilon} = \tilde{\varepsilon}(\boldsymbol{\varepsilon}) = \langle \mathbf{n}_\sigma \cdot \boldsymbol{\varepsilon} \rangle^+$. When the total energy available for the FE is dissipated (i.e. $D = 1$, D being the damage variable), it is declared cracked and its elementary stiffness matrix is set to zero (Tailhan et al 2010). This allows to avoid stress-locking phenomena;
2. The model is numerically implemented using a rotating crack approach (Rots et al 1985; Jirásek and Zimmermann 1998). During the dissipative phase (i.e. $D < 1$), the normal $\mathbf{n}_\sigma$ is allowed to evolve according to any changes in the stress state $\boldsymbol{\sigma}$ in the material. Only when the element is declared as cracked, the normal to the crack plane fixed: $\mathbf{n}^c = \mathbf{n}_\sigma$;
3. Differently from smeared-cracking approaches (De Borst and Nauta 1985; Jirsek 2011; Meschke et al 2011), no additive decomposition is introduced in the constitutive law to distinguish between elastic deformation and crack contributions. A elementary crack is supposed to exist only after the condition $D = 1$ is achieved (Rossi and Tailhan 2012). The elementary crack opening a_e is then computed from the projection of the elementary displacements along the direction of $\mathbf{n}^c$;
4. For sake of simplicity, crack re-closure is not explicitly treated. The model assumes that the dissipative process does not influence the elementary stiffness in compression. So, for reclosed cracks, the elementary stiffness matrix in compression is completely recovered while the elementary tensile strength f_t is set to zero.

2.3 Statistical model parameters

The constitutive law $(\boldsymbol{\sigma}, \boldsymbol{\varepsilon})$ is completely defined by two parameters: the tensile strength f_t and the volumetric density of dissipated energy g_c. An energetic regularisation technique allows to compute g_c from the surface cracking energy $\mathcal{G}_c$: $g_c = \mathcal{G}_c / l_e$ (Bazant and Oh 1983). The quantity l_e denotes the elementary characteristic length and is here computed from elementary volume as $l_e = V_e^{1/3}$. More complex definitions are possible, depending on the FE shape and the order of interpolation of the displacement field. This choice can influence the predicted crack paths, however due to the probabilistic aspects of the model this effect is strongly reduced.

Mechanical properties f_t and $\mathcal{G}_c$ are defined element-by-element according to spatially uncorrelated Weibull and lognormal statistical laws respectively (Feller 2008).

Due to the aforementioned modelling assumptions (Sec. 2.1), their statistical parameters depend on the elementary volume through the local heterogeneity ratio ξ_e. The only exception is the mean value of the energy distribution, which is assumed independent of ξ_e. Its value is estimated as $\mu_G = \mathcal{G}_c$, where $\mathcal{G}_c$ is the

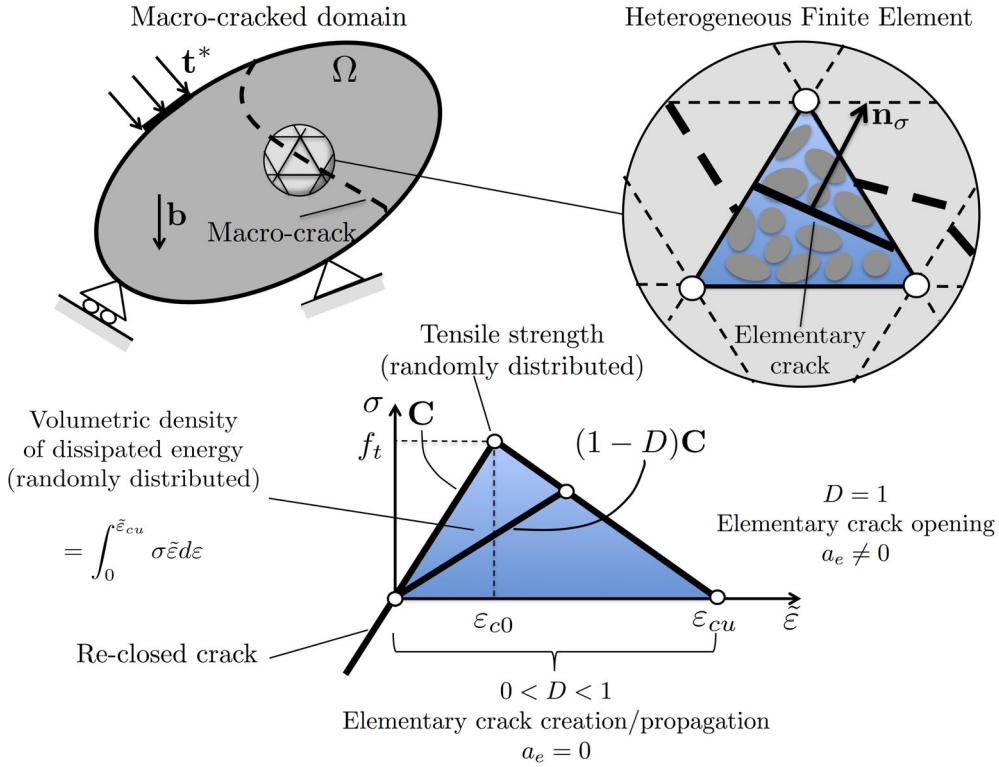

Fig. 1 Illustration of the main aspects of the proposed "semi-explicit" probabilistic cracking model.

critical strain energy release rate as defined in the context of the Linear Fracture Mechanics (LFM) by Irwin (1968). For the concrete formulation used herein (Tab. 1) its value has been experimentally obtained by Rossi (1988): $\mathcal{G}_c = 1.31410 \times 10^{-4}$MN/m.

Using $\mathcal{G}_c$ as model parameter instead of the fracture energy $\mathcal{G}_f$ (Hillerborg et al 1976), as stated by Non Linear Fracture Mechanics (NLFM) for quasi-brittle materials, is based on two strong physical assumptions (Rossi and Tailhan 2012; Tailhan et al 2013):

1. the Griffith's theory for brittle fracture is assumed valid at the FE level. According to this theory, $\mathcal{G}_c$ is proportional to the specific fracture energy per unit area γ, which is an intrinsic material parameter (e.g. in plane strain conditions: $\mathcal{G}_c = 2\gamma$). Therefore $\mathcal{G}_c$ can also be considered as such, at least in average value. This assumption is reasonable, in light of the experimental results obtained by Rossi (1988) and Rossi et al (1990);
2. due to the material heterogeneity the dissipated energy can undergo variations (dispersion in statistical terms) around the average value. This dispersion is considered as directly influenced by the size of the stressed volume (i.e. of the finite element), as this volume may (or may not) be concerned by the propagation of a crack. In particular, as qualitatively illustrated in Fig. 2, it should increase as ξ_e decreases and vice-versa.

Table 1 Ordinary concrete mix design.

Components	kg/m^3
Cement: CEM I 52.5 N PMES CP2	340
Water	184.22
Sand: Bernires 0/4	739.45
Gravels: Bernires 6.3/20	1072.14

The laws $b_s = b_s(\xi_e)$ and $c_s = c_s(\xi_e)$ defining shape and scale factors of the Weibull distribution for the tensile strength, as well as the variance $\eta_G = \eta_G(\xi_e)$ of the cracking energy distribution, have to be identified through an inverse analysis approach.

This calibration phase generally requires a large number of computations and is rather computationally expensive. However, once the statistical laws have been obtained for a given material, they can be directly used in other computations without any ajustements.

3 Fluid transfer in cracking concrete

To study the feasibility of the coupling between probabilistic cracking and fluid transfers in concrete, a simplified transfer model is considered. Concrete is treated as a saturated and initially isotropic porous medium,

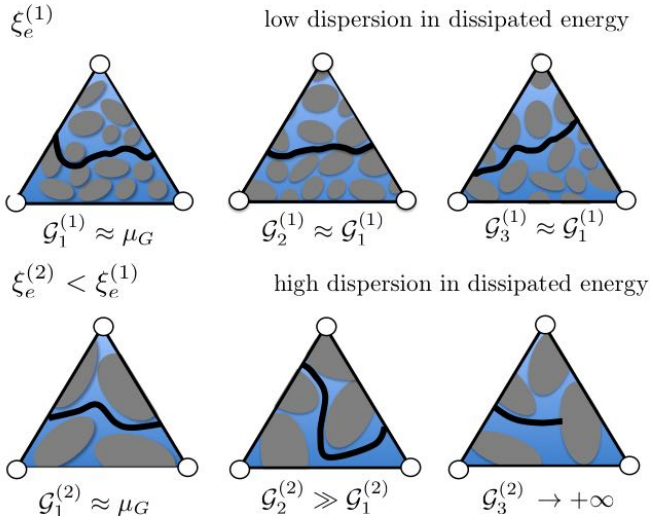

Fig. 2 Influence of the local heterogeneity ξ_e on the crack propagation on a heterogeneous volume element and influence on the cracking energy dispersion.

and the flow is assumed to be incompressible. Furthermore, the sole considered source of HM coupling is the influence of cracking on the local transfer properties.

Under these assumptions, transport problem is governed by the sole continuity equation of the fluid phase, and can be separately solved from the mechanical one. The numerical solution is obtained through a standard FEM formulation (Lewis and Schrefler 1987; Dal Pont et al 2007; Meftah et al 2012), using the same computational grid adopted in mechanical computations. The treatment of more complex thermo-hydraulic problems can be easily integrated using fully coupled staggered solution procedures (Meftah et al 2012).

3.1 Apparent permeability of the cracked element

Darcy-like fluid flows are assumed both in cracked and undamaged volume elements. In the absence of body forces and assuming a steady-stated, single-phase and laminar flow, the fluid specific mass flow rate $\mathbf{q}$ depends on the local pressure gradient ∇p according to the linear relation (Darcy 1856):

$$\mathbf{q} = \rho\,\mathbf{v} = -\rho\,\mu^{-1}\mathbf{k}\nabla p \tag{2}$$

where $\mathbf{v}$ is the mean fluid velocity, ρ is the fluid density, μ is its cinematic viscosity and $\mathbf{k}$ denotes the elementary permeability tensor.

For undamaged FEs, $\mathbf{k}$ coincides with the so-called intrinsic permeability tensor of the porous medium:

$$\mathbf{k} = \mathbf{k}^0 = k^0\mathbf{I} \tag{3}$$

where k^0 is the intrinsic permeability of the porous medium and $\mathbf{I}$ denotes the second order identity tensor.

Once a FE is cracked, the macro-crack represents a preferential pathway for the penetration of fluids. At the FE scale, this can be taken into account (Dormieux and Kondo 2004; Shao et al 2005; Meschke et al 2011) by introducing the non-isotropic "apparent" elementary permeability tensor:

$$\mathbf{k} = \mathbf{k}^0 + \mathbf{T}^t\mathbf{k}^c\mathbf{T} \tag{4}$$

where $\mathbf{k}^c$ is the cracking induced anisotropic contribution to the apparent permeability (written in the local reference system of the crack), and $\mathbf{T}$ is the rotation tensor. The term "apparent" is here used to remark that in presence of a localised/discrete cracks the rigorous definition of homogenised quantities (e.g. permeabilities) is not possible, as the assumption of statistical homogeneity (Freudenthal 1950; Hashin 1983; Drugan and Willis 1996; Ostoja-Starzewski 2002; Stroeven et al 2004) underlying the existence of a REV is not verified (Bodin et al 2003; Meftah et al 2012).

The crack contribution $\mathbf{k}^c$ figuring in Eq. (4) have to be properly defined, to take into account the loss of isotropy of the flow within a cracked area and to ensure the mesh objectivity of the simulated response. If one assumes that the crack does not modify the flow along the direction of $\mathbf{n}^c$ (Dormieux and Kondo 2004; Pouya and Ghabezloo 2010), the apparent permeability tensor $\mathbf{k}^c$ can be written as follows:

$$\mathbf{k}^c(a_e, \mathbf{n}^c) = k^c(a_e)\frac{a_e}{l_e}\left(\mathbf{I} - \mathbf{n}^c \otimes \mathbf{n}^c\right) \tag{5}$$

where $k^c = k^c(a_e)$ is the intrinsic crack permeability and l_e denotes the the elementary characteristic length for the hydraulic problem (estimated as in mechanical computations). From Eqs. (5) and (4) stems directly that when $a_e = 0$, the crack contribution vanishes. Therefore, no irreversible effects on local fluid flow due to residual cracks can be taken into account.

3.2 Crack permeability: experimental constitutive law

The intrinsic permeability of the crack k^c is conventionally estimated according to the so-called parallel plates model (Snow 1969). This conductivity model stems directly from the resolution of Navier-Stokes equations (Temam 2001) assuming that the fracture walls are two smooth and parallel plates, separated by an aperture a_e (Zimmerman and Bodvarsson 1996). Real cracks in concrete, however, have rough walls and variable apertures. In numerical modelling, some authors (Segura and Carol 2004; Secchi and Schrefler 2012) suggest to

correct the standard cubic law by introducing a phenomenological factor $\alpha > 1$ such that:

$$k^c = k^c(a_e) = \frac{a_e^2}{12\,\alpha} \tag{6}$$

The factor α is typically assumed constant, with values ranging between 10 and 1000 (Wang et al 1997; Picandet et al 2009; Akhavan et al 2012) depending on concrete formulations and adopted experimental procedures. However, as experimentally shown by Rastiello et al (2014), the parameter α could not be considered as a constant as it should decrease during the crack opening process. In particular, the following power-law relation can be used:

$$\alpha = \alpha(a) = \beta a^\gamma \tag{7}$$

where $\beta > 0$ and $\gamma < 0$ are two parameters depending on the crack geometry and, indirectly, on the concrete formulation. For the ordinary concrete formulation herein used (Tab. 1), the following values hold: $\beta = 5.625 \times 10^{-5}$ and $\gamma = -1.19$ (if a_e is expressed in metres).

Finally, combining Eqs. (7) and (6), the following constitutive law can be used in numerical computations:

$$k^c = \begin{cases} \frac{a_e^{2-\gamma}}{12\beta} & a_e < a_{e,t} \\ \frac{a_e^2}{12} & \text{otherwise} \end{cases} \tag{8}$$

where $a_{e,t}$ is the the crack opening such that the parallel plates model is recovered ($\alpha = 1$).

4 Coupling procedure

A Monte-Carlo like procedure is used to obtain a statistical description of the HM response of the analysed system. Under the aforementioned weak HM coupling assumption, the mechanical and hydraulic problems are sequentially solved (using two specialised and ad-hoc developed FE codes) as follows:

1. a series of mechanical simulations is performed to induce cracking and to estimate the structural mechanical response;
2. the local cracking informations (elementary openings a_e, cracks orientations $\mathbf{n}^c$) obtained in mechanical computations are used, in hydraulic computations, to define elementary apparent permeability tensors $\mathbf{k}$;
3. the transfer properties of the cracking structure are then statistically analysed and put into relation with mechanical fields.

In the following sections, the feasibility of the proposed modelling strategy is explored by simulating the HM splitting tests by Rastiello et al (2014), for estimating the real-time evolution of the transfer properties of a concrete sample under Brazilian loading. This study in performed in two phases:

1. purely mechanical experimental results are first used (Sec. 5) in order to identify the statistical parameters b_s, c_s and η_G (defined in Sec. 2.3) for two values of the elementary heterogeneity ratio:

$$\xi_e = 0.01 \quad \text{and} \quad \xi_e = 0.001\,; \tag{9}$$

2. in the second phase (Sec. 6), the calibrated parameters are used as input data in HM computations. These latter are performed using a FE mesh which is different from those used in previous phase. This allows to obtain a first validation of calibrated statistical parameters and, at the same time, an estimation of the model capabilities in predicting fluid transfers in cracking media.

5 Mechanical model parameters identification

Purely mechanical experimental results obtained by Rastiello et al (2014) on samples $d_s = 110\,\text{mm}$ in diameter and $t_s = 50\,\text{mm}$ in thickness are considered as reference data to perform a preliminary inverse analysis on the statistical parameters of the mechanical model. The choice of the optimal set of parameters is performed using a semi-automatic procedure, based on the comparison between the experimental and numerical global sample responses.

5.1 Numerical modelling of the Brazilian test

The mechanical response of a cylindrical sample under Brazilian loading is numerically simulated according to the proposed "semi-explict" cracking model.

Numerical computations are performed using two FE mesh (Fig. 4). They are composed respectively of 4250 and 13037 four-noded tetrahedral FEs with linear interpolation in the the displacement field. For both mesh, the central zones of the sample are discretised through structured grids composed by FEs with quasi-constant ξ_e values (i.e. elementary volumes).

The upper and lower steel bearing plates are represented through two linear elastic parallelepipeds b in width. Their presence allows to distribute external load over a finite width bearing strip and ensure to limit damage concentrations near the bearing surfaces (i.e. constrained nodes). It is well-known that, in Brazilian

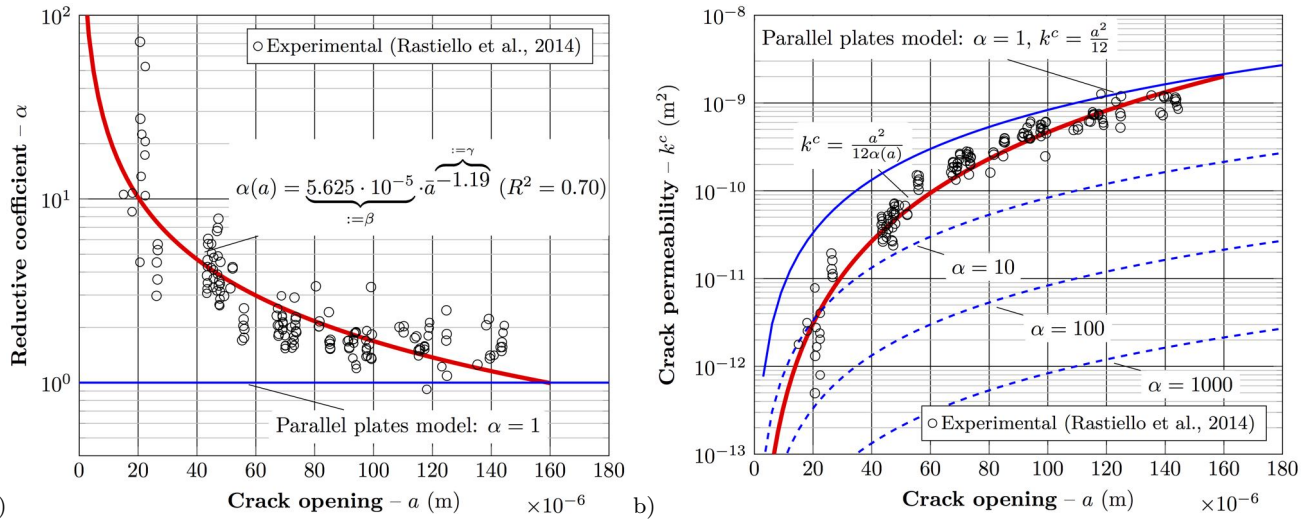

Fig. 3 Experimentally adapted parallel plates model (Eq. (8)).

tests, the b/d_s ratio sensibly influences the sample mechanical response and can induce scale effects (Rocco et al 1999a,b). However, the chosen width ($b = 1$ cm) is small enough to neglect its influence on the simulated response (Rastiello 2013) and, at the same time, it is completely representative of the experimentally observed contact areas between the bearing plates and the sample surfaces (Boulay et al 2009; Rastiello et al 2014).

Diametrical loading is simulated by imposing vertical displacements of the upper bearing strip. In analogy with the experiments, a indirectly controlled loading technique is used to avoid mechanical instabilities (snap-backs/through phenomena) in the phase post-peak of force. The vertical displacement increment at each loading step is then adjusted to ensure monotonically growing mean sample diameter variations Δd_s. These latter are computed as linear combination of the horizontal displacements of the four nodes representative of the real measurement points (Fig. 8). Numerically, this is obtained through the arc-length type algorithm (Riks 1979; Ramm 1981; Crisfield 1982) presented by Rastiello (2013).

In the following, in analogy with experiments, the mechanical response of the sample is represented through the average diameter variation of the sample Δd_s and the diametrical load F.

5.2 Parameters identification - global sample responses

Ten simulations for each set of parameters are performed. One can show that this represent a good compromise between CPU time and accuracy of the solution. Further increases in the number of simulations do not induce sensible variations in terms of mean sample response.

Based on the statistical interpretation of about 4000 computations, the following parameters have been finally chosen:

$$b_s = \begin{cases} 6.6, & \xi_e = 0.01 \\ 7.0, & \xi_e = 0.001 \end{cases} \qquad c_s = \begin{cases} 1.0, & \xi_e = 0.01 \\ 1.0, & \xi_e = 0.001 \end{cases} \tag{10}$$

$$\mu_g = \mathcal{G}_c \quad \forall\, \xi_e \quad \eta_G = \begin{cases} 7 \times \mathcal{G}_c, & \xi_e = 0.01 \\ 10 \times \mathcal{G}_c, & \xi_e = 0.001 \end{cases} \tag{11}$$

to obtain the tensile strength in MN and the cracking energy in MN/m. From parameters b_s and c_s is easy to compute, the mean values and the variance of the strength distribution (Feller 2008):

$$\mu_s = b_s\, \Gamma(1 + c_s^{-1}) \quad \eta_s^2 = b_s^2\, \Gamma(1 + 2c_s^{-1}) - \mu_s^2 \tag{12}$$

where Γ is the so-called gamma function.

The $(F, \Delta d_s)$ responses corresponding to the calibrated parameters are depicted in Fig. 5. A good agreement with experimental results can be put in evidence both in terms of mean values and dispersion. However, it is worth observing that numerical simulations cannot continue after Δd_s reaches the maximum value of 80μm (i.e. $< 300\mu$m experimentally analysed). For larger Δd_s levels, the iterative resolution algorithm fails to converge, due to the poor conditioning of the stiffness matrix, resulting from the presence of many cracked elements in the central zone of the specimen and/or to uncontrolled oscillations in elementary opening process.

It is worth observing that the unity value assigned to the shape factor of the Weibull law, for both ξ_e values, corresponds to the transition between lognormal and exponential distributions. This result is consistent with

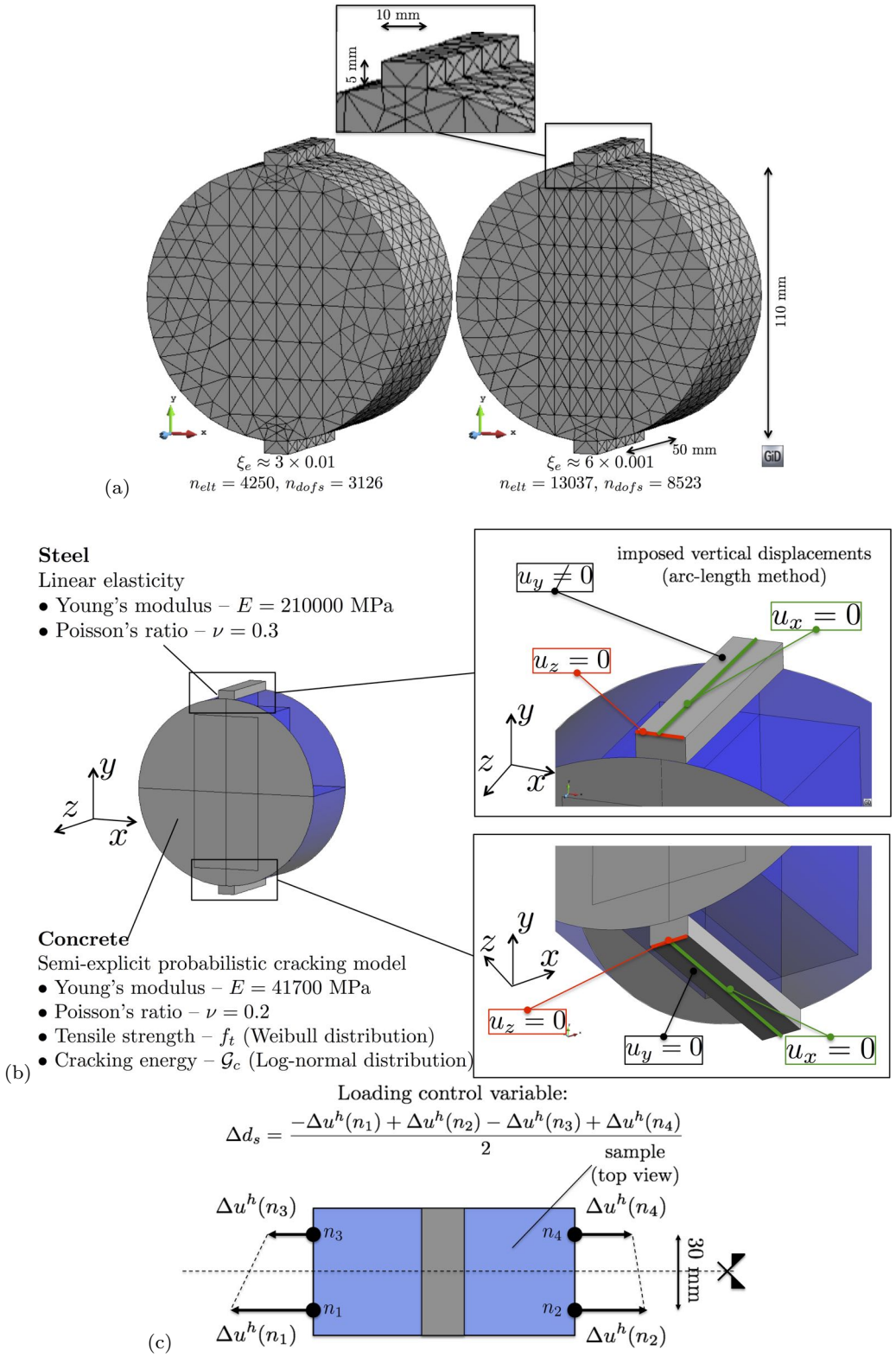

Fig. 4 a) Finite element mesh used to calibrate the statistical parameters of the mechanical model (inverse analysis), b) imposed boundary conditions, c) and definition of the loading control variable.

the results of the inverse analysis performed by Tailhan et al (2010) using a probabilistic elastic-brittle constitutive law. Furthermore, consistently with the main modelling assumptions, the variance of the energy dis-

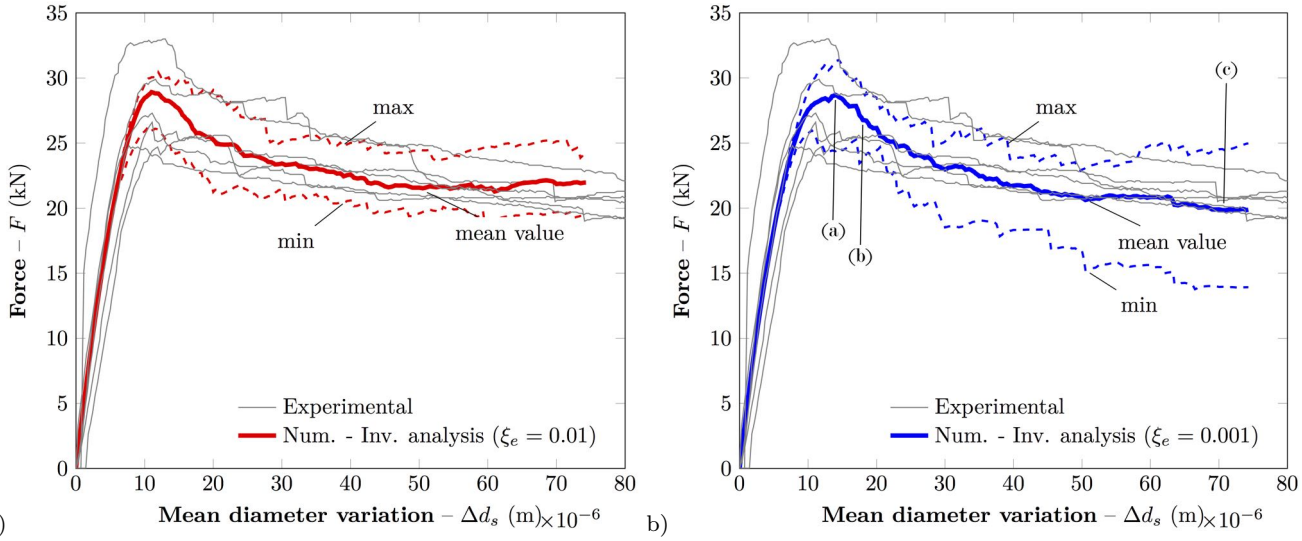

Fig. 5 Global $(F, \Delta d_s)$ responses obtained through the two FE mesh using the chosen statistical parameters, with approximative identification of the loading levels corresponding to the crack distributions and displacement fields depicted in Fig. 6.

tribution increases with the elementary heterogeneity ξ_e.

5.3 Local informations: crack openings

Figure 6 represents the horizontal displacement fields and elementary cracks distributions for three phases of a representative test. Numerical results put in evidence that: (1) in the pre-peak load phase, the deformation process between the two faces of the sample remains symmetric and the stress/strain fields are well approximated by standard elastic solutions (Timoshenko and Goodier 1951); (2) once the peak of load is attained, the crack opening process become strongly un-symmetric. Crack localisation starts on one face of the sample and rapidly propagates to the other one. The deformation field then localises in a band of width approximately equal to the size of one element. As experimentally observed by Rastiello et al (2014), in this phase the sample is split into two undamaged quasi-elastic blocks. From a qualitative point of view the computed displacement fields are very similar to those obtained by Rastiello et al (2014) using a digital imaging correlation technique.

A good agreement between numerical and experimental results can be observed also in quantitative terms. In Fig. 7 the comparison is established in terms of mean crack opening a_m at mid-height of the plane faces of the sample. For both sides of the sample, crack apertures are numerically computed as follows. In a first step, the position of the "crack" is obtained from the displacement field corresponding to the last loading step. In a second step the crack aperture $a_{\mathrm{m,f(r)}}$ at mid-height of the sample is computed as the relative displacement of the two nodes disposed on the opposite sides of the crack. As these nodes share two FEs, a crack is considered as present (i.e. $a_{\mathrm{m,f(r)}} \neq 0$) only if both the elements are cracked. Otherwise $a_{\mathrm{m,f(r)}} = 0$. Finally, the mean crack opening is computed as $a_\mathrm{m} = (a_{\mathrm{m,f}} + a_{\mathrm{m,r}})/2$.

For both mesh, once a macro-crack develops into the sample, the relation $(a_\mathrm{m}, \Delta d_s)$ is pseudo-linear as in experiments.

6 Hydro-mechanical computations

The complete HM splitting test is modelled in this section. The statistical parameters calibrated in Sec. 5, are used as input data of the mechanical model. However, due to the variable dimensions of the FEs ensuring the spatial discretisation of the sample, linear functions of ξ_e are used to define $b_s = b_s(\xi_e)$, $c_s = c_s(\xi_e)$ and $\eta_G = \eta_G(\xi_e)$ (Sec. 2.3).

6.1 Numerical modelling of the HM test

The real-time evolution of the transfer properties of a cylindrical sample under loading is numerically simulated. The FE mesh adopted in computations is depicted in Fig. 8. It is composed of approximately 44000 tetrahedral finite elements with linear interpolations of nodal displacements and pressures.

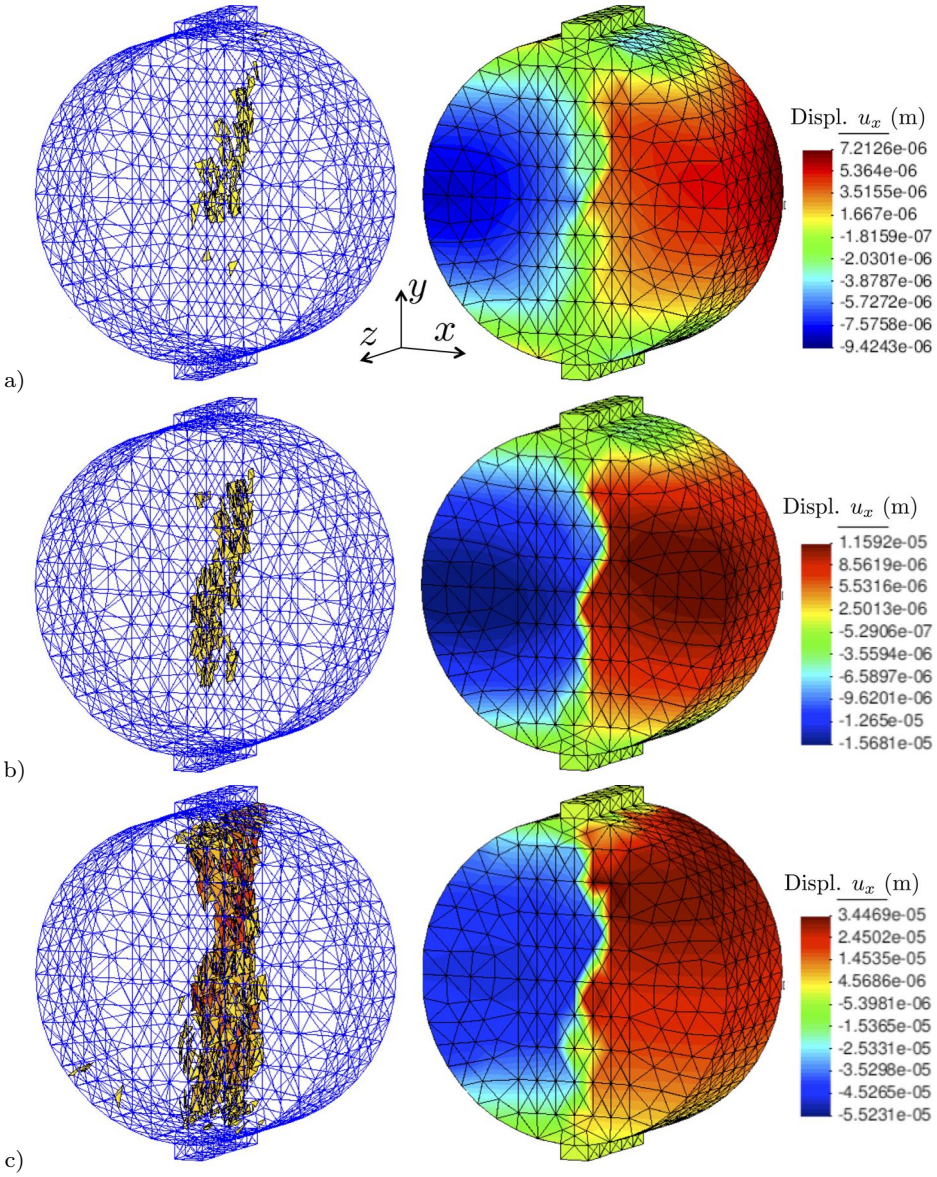

Fig. 6 Displacement fields and crack distributions inside the sample for three phases of a representative numerically simulated Brazilian test.

The mechanical loading is performed according the numerical procedure presented in previous section. Concerning the hydraulic boundary conditions, two constant fluid pressure distributions $p^{in(out)}$ are applied on two circular plane surfaces $S^{in(out)}$ of the sample in real-time with the mechanical load. Their diameter $d = 0.077\,\mathrm{m}$ is equal to those of the silicone joints experimentally adopted in order to ensure the absence of leaks at the contact between the experimental equipment and the sides of the sample. More details are given in Rastiello et al (2014).

6.2 Representative transfer variables

The hydraulic response of the sample is represented through the sample transmissivity T_{num}.

Under the assumption of unidirectional flow between the two plane faces of the sample, it is obtained at each calculation step as:

$$T_{num} = -Q_{num}\frac{\mu}{\rho}\left[\frac{\Delta p}{t_s}\right]^{-1} \tag{13}$$

where Q_{num} is the mass flow rate (computed at the outlet/inlet section) and Δp is the differential pressure.

The comparison of T_{num} with the homologous experimentally obtained quantity call for some considerations. Due to the saturated and laminar flow conditions,

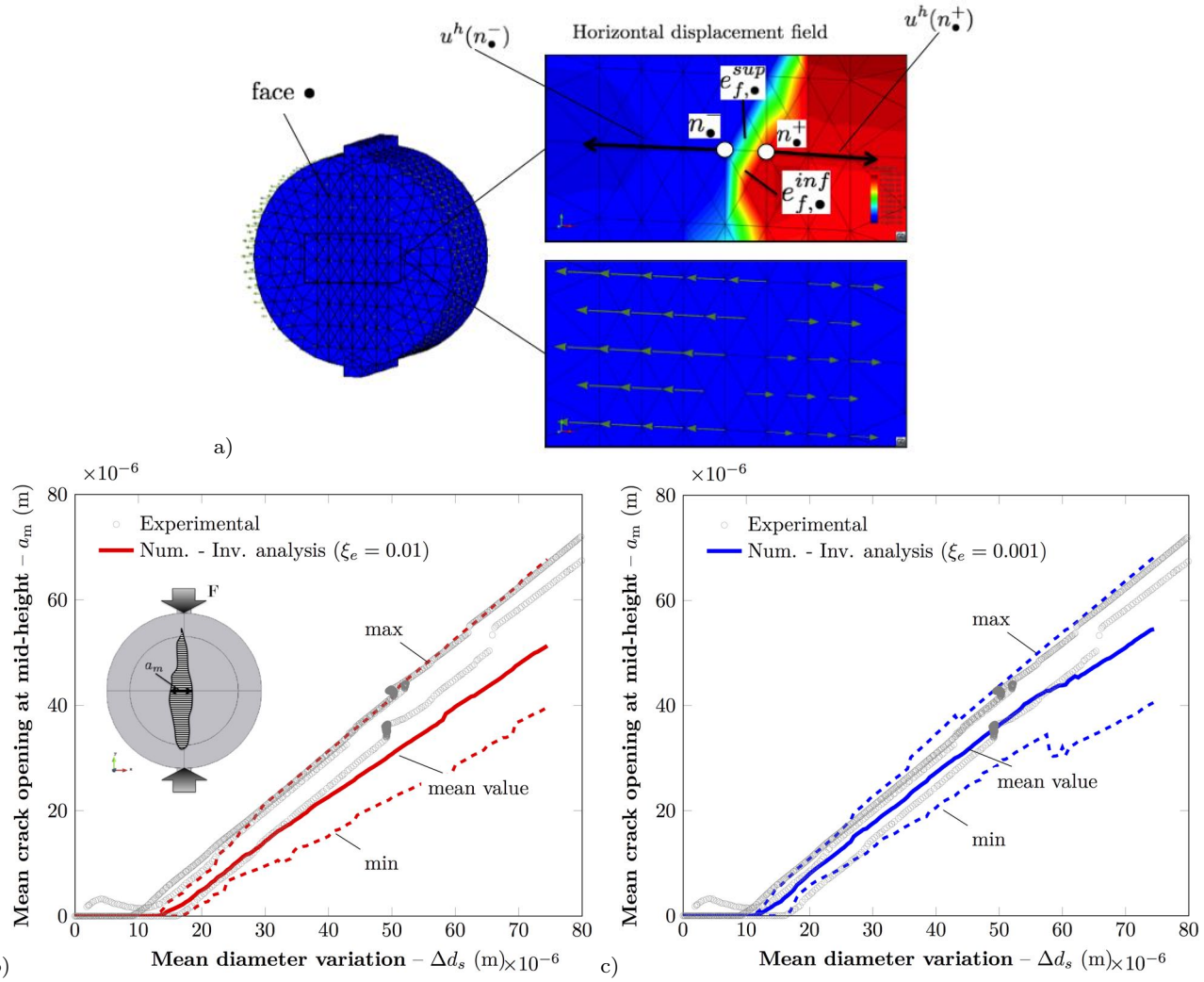

Fig. 7 Procedure to compute crack opening displacement at mid-height of the sample a_m from displacement field and comparison between numerically computed and experimentally obtained $(a_\mathrm{m}, \Delta d_s)$ relationships.

the total transmissivity T_{num} can be additively decomposed as follows:

$$T_{num} = T^0_{num} + T^c_{num} \tag{14}$$

where T^0_{num} is the contribution of the flow through the porous medium and T^c_{num} is those corresponding to the crack flow. In all rigour, this quantity is not directly comparable to experimental one, as in this case only the crack contribution T^c_{exp} is known. The comparison is however possible if one observes that due to the low permeability of the material ($k^0 \approx 10^{-21}\mathrm{m}^2$ (Baroghel-Bouny et al 2011)), the crack contribution to the mass flow rate is several times greater than those associated to the porous medium ($T^0_{num} \approx 10^{-24}\mathrm{m}^4$), already for very small crack openings. Therefore: $T_{exp} \approx T^c_{exp}$.

6.3 Numerical results

The mean $(F, \Delta d_s)$ and $(T_{num}, \Delta d_s)$ responses, computed over ten mechanical and hydraulic simulations, are represented in Fig. 9. The crack distributions and the fluid flow fields for three phases of a representative test are depicted in Fig. 10.

During the test, sample transmissivity T_{num} evolves according two main phases: (1) For low Δd_s levels ($< 15\,\mu$m), approximately up to the the peak force, the sample transmissivity T_{num} remains almost constant ($T_{num} = T^0_{num}$). This condition does not correspond to the absence of cracks in the sample, as isolated elementary cracks may be present already for moderate loading levels. However, their contribution to T_{num} remains negligible ($T^c_{num} < T^0_{num}$). It is worth observing that this behaviour should not be interpreted as a numerical evidence of the existence of threshold crack

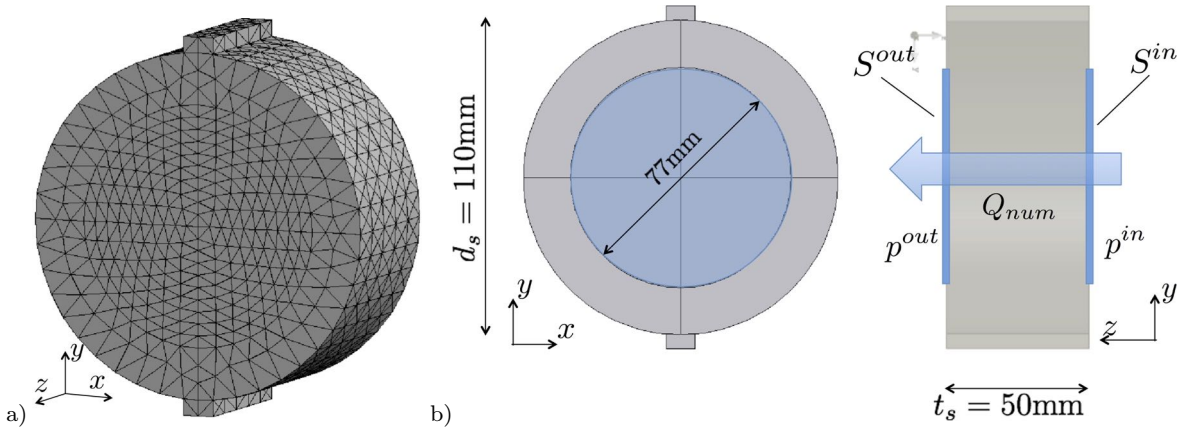

Fig. 8 a) Finite element mesh used in HM computations and b) hydraulic boundary conditions.

opening beyond which the water flux is not influenced by the crack (Wang et al 1997; Aldea et al 2000), as a a unique macro-crack (i.e. continuous flowing path) is not yet present in the specimen and a crack opening can not be defined; (2) Once the peak load is attained, a macro-crack propagates through the specimen. Due to the creation of this preferential flow path, T_{num} rapidly increases by several orders of magnitude. Numerical results tends to overestimate the experimental transmissivity values ($T_{num} > T_{exp}$). This is partly due to the fact that the experimentally adapted parallel plates model (Eq. (7)) is strictly valid only in the range of experimentally explored crack apertures ($20\mu\text{m} < a < 160\mu\text{m}$). Therefore, the extrapolation of these results to thinner cracks ($a < 20\mu\text{m}$) calls for further confirmations. From the numerical point of view, a further cause for over-estimation may be associated with the possible presence of adjacent cracked FEs. In this case, each FE contributes to the T_{num} in proportion to the third power of its own crack opening.

A good agreement between numerical and experimental results can be put in evidence both in terms of mechanical and hydraulic responses. The comparison among the mechanical responses obtained in this series of analysis and those previously obtained using different FE mesh, provides a further confirmation of the independence of the global simulated response with respect to the computational grid. Due to the aforementioned difficulties in simulating Brazilian tests, a complete validation of the proposed modelling approach can not be obtained. One can however show that the simulated responses are completely comparable to the experimental ones, at least in terms of tendency, over the whole range of experimentally explored Δd_s.

7 Conclusions

A numerical finite element study on fluid leakage in cracking concrete has been presented. Concrete cracking is modelled through a macroscopic ("semi-explicit") probabilistic model. Material heterogeneity is taken into account through the use of statistical distributions of mechanical properties (tensile strength and cracking energy) (Rossi and Wu 1992; Rossi et al 1996; Tailhan et al 2010, 2012, 2013). Cracking is treated element-by-element without an explicit definition of a propagation criterion. In this approach, macro-cracks results from the progressive and random creation of elementary cracks. The main physical assumption is that each FE represents a volume of heterogeneous material (Rossi and Wu 1992; Tailhan et al 2010), whose mechanical behaviour is controlled by its own heterogeneity degree $\xi_e = V_e/V_g$ (i.e. the ratio of the elementary volume V_e to a volume representative of the heterogeneity of the material V_g). In the present formulation, it is assumed that the cracking process (i.e. the creation and propagation of a crack within the element itself) induces some local energy dissipation. This dissipative process is mathematically represented through a probabilistic isotropic damage model (Lemaitre and Chaboche 1994). According to the aforementioned modelling assumption, material properties (strength and fracture energy) are defined element-by-element according to spatially uncorrelated random fields. Their statistical parameters are defined for each element depending on its own elementary volume (V_e) according to experimentally validated laws.

The cracking-transfer coupling is treated as weak. It is assumed that the cracking of the FE, of mechanical origin, induces a loss of isotropy of its own apparent permeability tensor. The use of an experimentally modified parallel plates model (Rastiello et al 2014) allows to

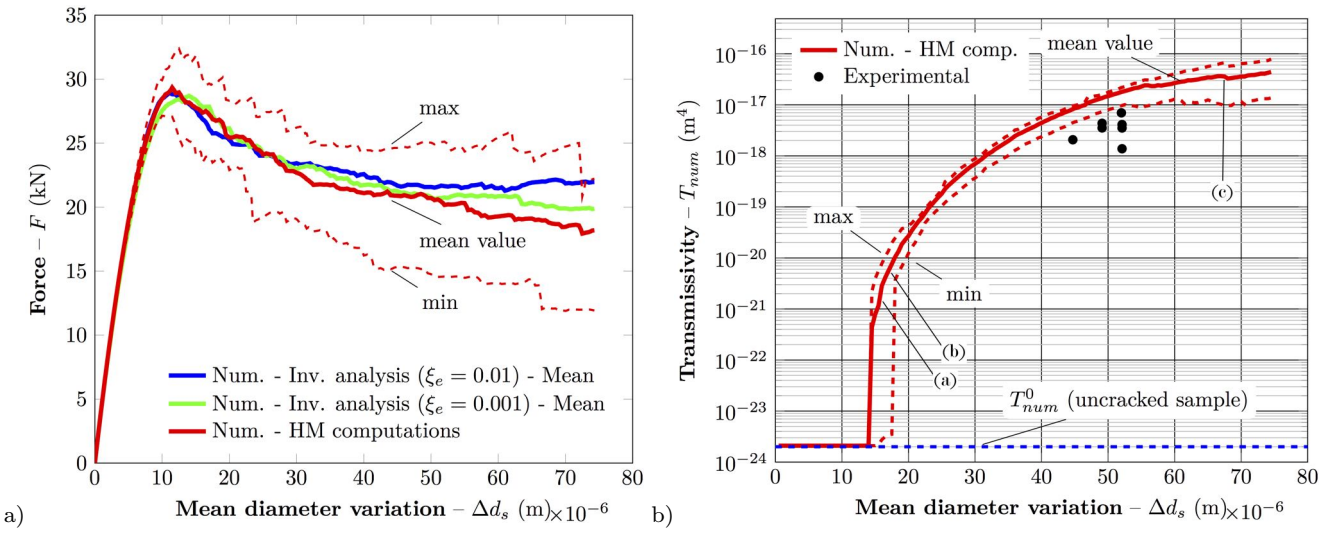

Fig. 9 $(F, \Delta d_s)$ and $(T_{num}, \Delta d_s)$ responses for the whole hydro-mechanical series of computations, and approximative identification of the simulation steps corresponding to the crack distributions and fluid flow fields depicted in Fig. 10

compute the crack permeability, macroscopically taking into account the main causes of the deviation between the idealised Pouiselle-like flow and the flow in real cracks (Zimmerman and Bodvarsson 1996).

A probabilistic Monte-Carlo type approach allows to statistically validate the numerical results.

The feasibility of the proposed modelling strategy is explored by simulating the HM splitting tests developed by Rastiello et al (2014), for mass flow rate measurements through concrete samples under Brazilian loading. Experimental results have been first used to identify the statistical parameters of the mechanical model for two ξ_e values. Then, the calibrated parameters have been used as input data in HM computations. Numerical results provided two kinds of informations. The first-one concerns the relevance of the mechanical model in predicting cracking. The second-one, concerns a verification of the validity of the coupling strategy in estimating fluid leakage in cracking concrete (at least at the sample scale). This second aspect represents a further indirect verification of the adequacy of the mechanical model in a "fine" description of cracking. According to the theoretical predictions, the laminar flow through a crack is indeed completely determined by the geometry of the crack itself. Therefore, an accurate prediction of the fluid flow rate through the cracking sample can be interpreted as an indicator of the level of accuracy (at least in statistical terms) of the model in predicting local cracks informations (i.e. openings, spatial distribution of the local apertures).

Further research are needed to validate the model at a structural scale. Furthermore, the complexity of the transfer model should be increased by taking into account compressible flows (e.g. air), partially saturated conditions and stronger HM couplings. These aspects are important in modelling of cracking at a early-age (Ulm and Coussy 1998; Sellier et al 2010; Briffaut et al 2011), concrete behaviour at high temperatures (Gawin et al 1999; Dal Pont and Ehrlacher 2004; Meftah et al 2012), hydraulic fracturing (Ng and Small 1999; Carrier and Granet 2011; Secchi and Schrefler 2012).

References

Akhavan A, Shafaatian S, Rajabipour F (2012) Quantifying the effects of crack width, tortuosity, and roughness on water permeability of cracked mortars. Cement and Concrete Research 42(2):313–320

Aldea C, Ghandehari M, Shah S, Karr A (2000) Estimation of water flow through cracked concrete under load. ACI Materials Journal 97(5):567–575

Andrade C, Gonzalez J (2004) Quantitative measurements of corrosion rate of reinforcing steels embedded in concrete using polarization resistance measurements. Materials and Corrosion 29(8):515–519

Barani O, Khoei A, Mofid M (2011) Modeling of cohesive crack growth in partially saturated porous media; a study on the permeability of cohesive fracture. International Journal of Fracture 167(1):15–31

Baroghel-Bouny V, Kinomura K, Thiery M, Moscardelli S (2011) Easy assessment of durability indicators for service life prediction or quality control of concretes with high volumes of supplementary cementitious materials. Cement and Concrete Composites 33:832–847

Bary B (1996) Etude du couplage hydraulique-mécanique dans le béton endommagé. PhD thesis, Université Paris 6

Bazant Z, Oh B (1983) Crack band theory for fracture of concrete. Materials and structures 16(3):155–177

Bodin J, Delay F, De Marsily G (2003) Solute transport in a single fracture with negligible matrix permeability: 1. fundamental mechanisms. Hydrogeology journal 11(4):418–433

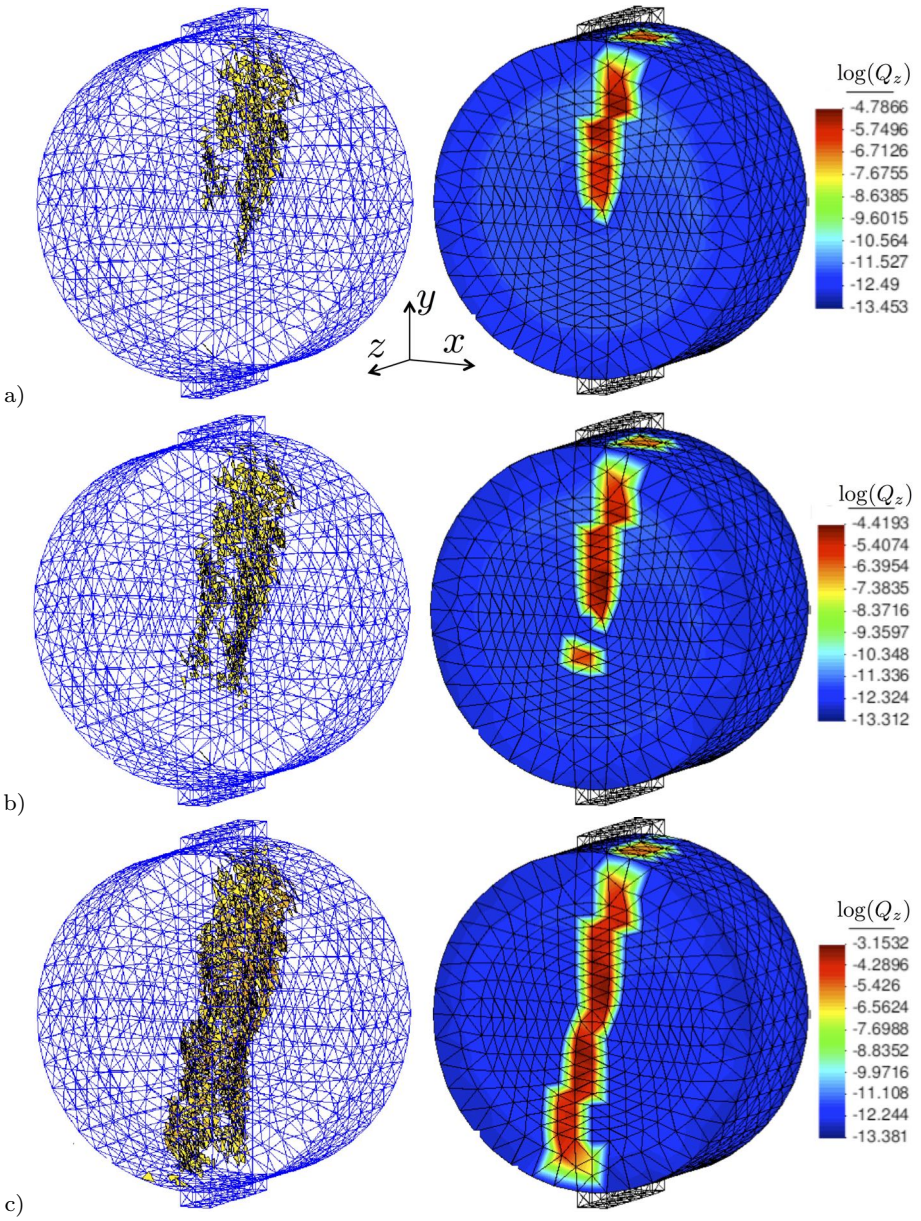

Fig. 10 Distribution of cracked FEs and fluid flow field computed for three phases of a representative hydro-mechanical Brazilian test.

Boulay C, Dal Pont S, Belin P (2009) Real-time evolution of electrical resistance in cracking concrete. Cement and Concrete Research 39:825–831

Briffaut M, Benboudjema F, Torrenti J, Nahas G (2011) Numerical analysis of the thermal active restrained shrinkage ring test to study the early age behavior of massive concrete structures. Engineering structures 33(4):1390–1401

Callari C, Armero F (2002) Finite element methods for the analysis of strong discontinuities in coupled poro-plastic media. Computer Methods in Applied Mechanics and Engineering 191(39):4371–4400

Carrier B, Granet S (2011) Numerical modeling of hydraulic fracture problem in permeable medium using cohesive zone model. Engineering Fracture Mechanics 79:312–328

Colliat JB, Hautefeuille M, Ibrahimbegovic A, Matthies H (2007) Stochastic approach to size effect in quasi-brittle materials. Comptes Rendus Mécanique 335(8):430–435

Coussy O (2004) Poromechanics. John Wiley & Sons

Crisfield M (1982) Accelerated solution techniques and concrete cracking. Computer methods in applied mechanics and engineering 33(1):585–607

Dal Pont S, Ehrlacher A (2004) Numerical and experimental analysis of chemical dehydration, heat and mass transfers in a concrete hollow cylinder submitted to high temperatures. International journal of heat and mass transfer 47(1):135–147

Dal Pont S, Schrefler B, Ehrlacher A (2005) Experimental and finite element analysis of a hollow cylinder submitted to high temperatures. Materials and Structures 38(7):681–690

Dal Pont S, Durand S, Schrefler B (2007) A multiphase thermo-hydro-mechanical model for concrete at high

temperaturesfinite element implementation and validation under loca load. Nuclear Engineering and Design 237(22):2137–2150

Darcy H (1856) Les Fontaines Publiques de la Ville de Dijon. Dalmont, Paris

De Borst R, Nauta P (1985) Non-orthogonal cracks in a smeared finite element model. Engineering Computations 2(1):35–46

Dormieux L, Kondo D (2004) Approche micromcanique du couplage permabilit–endommagement. Comptes Rendus Mecanique 332(2):135–140

Drugan W, Willis J (1996) A micromechanics-based nonlocal constitutive equation and estimates of representative volume element size for elastic composites. Journal of the Mechanics and Physics of Solids 44(4):497–524

Feller W (2008) An introduction to probability theory and its applications, vol 2. John Wiley & Sons

Freudenthal A (1950) The inelastic behavior of engineering materials and structures. Wiley

Gawin D, Majorana C, Schrefler B (1999) Numerical analysis of hygro-thermal behaviour and damage of concrete at high temperature. Mechanics of Cohesive-frictional Materials 4(1):37–74

Gawin D, Pesavento F, Schrefler B (2002) Simulation of damage–permeability coupling in hygro-thermo-mechanical analysis of concrete at high temperature. Communications in numerical methods in engineering 18(2):113–119

Granger L, Rieg C, Touret J, Fleury F, Nahas G, Danisch R, Brusa L, Millard A, Laborderie C, Ulm F, Contri P, Schimmelpfennig K, Barr F, Firnhaber M, Gauvain J, Coulon N, Dutton L, Tuson A (2001) Containment evaluation under severe accidents (cesa): synthesis of the predictive calculations and analysis of the first experimental results obtained on the civaux mock-up. Nuclear Engineering and Design 209(1-3):155 – 163

Hashin Z (1983) Analysis of composite materials. J appl Mech 50(2):481–505

Hillerborg A, Modeer M, Petersson PE (1976) Analysis of crack formation and crack growth in concrete by means of fracture mechanics and finite elements. Cement and concrete research 6(6):773–781

Ibrahimbegovic A, Colliat JB, Hautefeuille M, Brancherie D, Melnyk S (2011) Probability based size effect representation for failure in civil engineering structures built of heterogeneous materials. In: Papadrakakis M, Stefanou G, Papadopoulos V (eds) Computational Methods in Stochastic Dynamics, Computational Methods in Applied Sciences, vol 22, Springer Netherlands, pp 291–313

Irwin G (1968) Linear fracture mechanics, fracture transition, and fracture control. Engineering Fracture Mechanics 1(2):241–257

Jirásek M, Zimmermann T (1998) Rotating crack model with transition to scalar damage. Journal of engineering mechanics 124(3):277–284

Jirsek M (2011) Damage and smeared crack models. In: Hofstetter G, Meschke G (eds) Numerical Modeling of Concrete Cracking, CISM International Centre for Mechanical Sciences, vol 532, Springer Vienna, pp 1–49

Jourdain X, Colliat JB, DeSa C, Benboudjema F, Gatuingt F (2014) Upscaling permeability for fractured concrete: mesomacro numerical approach coupled to strong discontinuities. International Journal for Numerical and Analytical Methods in Geomechanics 38(5):536–550, DOI 10.1002/nag.2223

Larsson J, Larsson R (2000) Finite-element analysis of localization of deformation and fluid pressure in an elastoplastic porous medium. International journal of solids and structures 37(48):7231–7257

Lemaitre J, Chaboche JL (1994) Mechanics of solid materials. Cambridge university press

Lewis R, Schrefler B (1987) The finite element method in the deformation and consolidation of porous media. John Wiley and Sons Inc., New York, NY

Meftah F, Dal Pont S, Schrefler B (2012) A three-dimensional staggered finite element approach for random parametric modeling of thermo-hygral coupled phenomena in porous media. International Journal for Numerical and Analytical Methods in Geomechanics 36(5):574–596

Meschke G, Grasberger S, Becker C, Jox S (2011) Numerical Modeling of Concrete Cracking, Springer, chap Smeared Crack and X-FEM Models in the Context of Poromechanics, pp 265–327

Millard A, L'Hostis V (2012) Modelling the effects of steel corrosion in concrete, induced by carbon dioxide penetration. European Journal of Environmental and Civil Engineering 16(3-4):375–391

Montemor M, Simoes A, Ferreira M (2003) Chloride-induced corrosion on reinforcing steel: from the fundamentals to the monitoring techniques. Cement and Concrete Composites 25(4):491–502

Ng A, Small J (1999) A case study of hydraulic fracturing using finite element methods. Canadian geotechnical journal 36(5):861–875

Ostoja-Starzewski M (2002) Microstructural randomness versus representative volume element in thermomechanics. Transactions American Society of Mechanical Engineers – Journal of Applied Mechanics 69(1):25–35

Picandet V (2001) Influence d'un endommagement mécanique sur la perméabilité et la diffusivité hydrique des bétons. PhD thesis, LGC, Nantes

Picandet V, Khelidj A, Bellegou H (2009) Crack effects on gas and water permeability of concretes. Cement and Concrete Research 39(6):537 – 547

Pijaudier-Cabot G, Dufour F, Choinska M (2009) Permeability due to the increase of damage in concrete: From diffuse to localized damage distributions. Journal of engineering mechanics 135(9):1022–1028

Pouya A, Ghabezloo S (2010) Flow around a crack in a porous matrix and related problems. Transport in porous media 84(2):511–532

Ramm E (1981) Strategies for tracing the nonlinear response near limit points. Springer

Rastiello G (2013) Influence de la fissuration sur le transfert de fluides dans les structures en béton. stratégies de modeélisation probabiliste et eétude expeérimentale. PhD thesis, Université Paris-Est

Rastiello G, Boulay C, Dal Pont S, Tailhan J, Rossi P (2014) Real-time water permeability evolution of a localized crack in concrete under loading. Cement and Concrete Research 56(0):20 – 28, DOI http://dx.doi.org/10.1016/j.cemconres.2013.09.010

Réthoré J, De Borst R, Abellan MA (2007) A two-scale approach for fluid flow in fractured porous media. International Journal for Numerical Methods in Engineering 71(7):780–800

Riks E (1979) An incremental approach to the solution of snapping and buckling problems. International Journal of Solids and Structures 15(7):529–551

Rocco C, Guinea G, Planas J, Elices M (1999a) Size effect and boundary conditions in the brazilian test: Experimental

verification. Materials and Structures 32(3):210–217
Rocco C, Guinea G, Planas J, Elices M (1999b) Size effect and boundary conditions in the brazilian test: theoretical analysis. Materials and Structures 32(6):437–444
Rossi P (1988) Fissuration du béton: du matériau à la structure à l'application de la mécanique linéaire de la rupture. PhD thesis, cole Nationale des Ponts et Chausses
Rossi P, Tailhan J (2012) Cracking of concrete structures: interest and advantages of the probabilistic approaches. In: Rilem International Conference on Numerical Modelling Strategies for Sustainable Concrete Structures, SSCS'2012, Aix-en-Provence, France
Rossi P, Wu X (1992) Probabilistic model for material behavior analysis and appraisement of concrete structures. Magazine of Concrete Research 44:271280
Rossi P, Bruhwiler E, Chhuy S, Jenq Y, Shah S (1990) Fracture properties of concrete as determined by means of wedge splitting tests and tapered double cantilever beam tests. In: Shah S, Carpinteri A (eds) Fracture mechanics test methods for concrete, RILEM report 5, CRC Press, pp 87–128
Rossi P, Wu X, Le Maou F, Belloc A (1994) Scale effect on concrete in tension. Materials and Structures 27(8):437–444
Rossi P, Ulm F, Hachi F (1996) Compressive behavior of concrete: physical mechanisms and modeling. Journal of Engineering Mechanics 122(11):1038–1043
Rots J, Nauta P, Kuster G, Blaauwendraad J (1985) Smeared crack approach and fracture localization in concrete. HERON 30(1)
Secchi S, Schrefler B (2012) A method for 3-d hydraulic fracturing simulation. International Journal of Fracture 178(1-2):245–258
Segura J, Carol I (2004) On zero-thickness interface elements for diffusion problems. International journal for numerical and analytical methods in geomechanics 28(9):947–962
Sellier A, La Borderie C, Torrenti J, Mazars J (2010) The french national project ceos. fr: Assessment of cracking risks for special concrete structures under tchm stresses. In: Sixth International Conference on Concrete under Severe Conditions: Environment and Loading
Shao J, Zhou H, Chau K (2005) Coupling between anisotropic damage and permeability variation in brittle rocks. International journal for numerical and analytical methods in geomechanics 29(12):1231–1247
Simon H, Nahas G, Coulon N (2007) Airsteam leakage through cracks in concrete walls. Nuclear Engineering and Design 237(1517):1786 – 1794, nURETH-11 11th International Topical Meeting on Nuclear Reactor Thermal Hydraulics
Snow D (1969) A parallel plate model of permeable fractured media. PhD thesis, University of California at Berkley
Stroeven M, Askes H, Sluys L (2004) Numerical determination of representative volumes for granular materials. Computer Methods in Applied Mechanics and Engineering 193(3032):3221 – 3238, DOI 10.1016/j.cma.2003.09.023, ¡ce:title¿Computational Failure Mechanics¡/ce:title¿
Su X, Yang Z, Liu G (2010) Monte carlo simulation of complex cohesive fracture in random heterogeneous quasi-brittle materials: A 3d study. International Journal of Solids and Structures 47(17):2336–2345
Syroka-Korol E, Tejchman J, Mrz Z (2013) Fe calculations of a deterministic and statistical size effect in concrete under bending within stochastic elasto-plasticity and non-local softening. Engineering Structures 48(0):205 – 219, DOI 10.1016/j.engstruct.2012.09.013
Tailhan JL, Dal Pont S, Rossi P (2010) From local to global probabilistic modeling of concrete cracking. Annals of Solid and Structural Mechanics 1(2):103–115
Tailhan JL, Rossi P, Phan T, Foulliaron J (2012) Probabilistic modelling of crack creation and propagation in concrete structures: some numerical and mechanical considerations. In: SSCS-2012
Tailhan JL, Rossi P, Phan T, Rastiello G, Foulliaron J (2013) Multiscale probabilistic approaches and strategies for the modelling of concrete. In: FRAMCOS-8
Temam R (2001) Navier-Stokes equations: theory and numerical analysis, vol 343. American Mathematical Society
Timoshenko S, Goodier J (1951) Theory of elasticity. New York: McGraw-Hill
Ulm F, Coussy O (1998) Couplings in early-age concrete: from material modeling to structural design. International Journal of Solids and Structures 35(31):4295–4311
Wang K, Jansen D, Shah S, Karr A (1997) Permeability study of cracked concrete. Cement and Concrete Research 27(3):381–393
Weibull W (1951) A statistical distribution function of wide applicability. Journal of applied mechanics 18(3):293–297
Zimmerman R, Bodvarsson G (1996) Hydraulic conductivity of rock fractures. Transport in Porous Media 23:1–30